

1 **Editor summary:**

2
3 By analyzing the genome of over 9000 pig-associated isolates, this study shows that modernized agricultural systems have favored the
4 acquisition of antimicrobial resistance genes, population expansion and global transmission of pig-enriched Salmonella over the past
5 century.
6
7

8 **Peer Review Information:**

9 *Nature Food* thanks Séamus Fanning, Nabil-Fareed Alikhan and the other, anonymous, reviewer(s) for their contribution to the peer
10 review of this work.
11
12

13 **1. Extended Data**

Figure or Table # Please group Extended Data items by type, in sequential order. Total number of items (Figs. + Tables) must not exceed 10.	Figure/Table title One sentence only	Filename Whole original file name including extension. i.e.: Smith_ED_Fig1.jpg	Figure/Table Legend If you are citing a reference for the first time in these legends, please include all new references in the main text Methods References section, and carry on the numbering from the main References section of the paper. If your paper does not have a Methods section, include all new references at the end of the main Reference list.
Extended Data Fig. 1	Circular presentation of the maximum-likelihood phylogeny in Figure 1A.	Extended_Data_Fig_1 .eps	Outer rings: The clade, source, and geographic origin of each strain. Colored arcs underneath the tree show the cluster assignments as in the Key.
Extended Data Fig. 2	Evaluation of the presence of temporal signal in <i>S. enterica</i> serovar Choleraesuis.	Extended_Data_Fig_2 .eps	The analysis was performed on 587 genomes. (A) Linear regression between root-to-tip distances of strains and the sampling years with a coefficient of determination (R^2) of 0.67. (B) Substantially lower R^2 values were obtained for ten date-randomisation datasets. (C) The average (dots) and standard deviation (error bars) of the substitution rates for actual data

			(black) and ten date-randomization datasets (red), estimated by BactDating.
Extended Data Fig. 3	Assessing the existence of temporal signal randomization test in pig-enriched ceBGs	Extended_Data_Fig_3 .eps	(A) Coefficients of determination (R^2) for the ten date-randomisation tests were obtained by linear regression between root-to-tip distances of strains and the sampling years in pig-enriched ceBGs. (B) The average (dots) and standard deviations (error bars) of the substitution rates for actual data (black) and ten date-randomization datasets (red) by BactDating. Pig-enriched ceBGs including ceBG3 (n=3136), ceBG10 (n=622), ceBG17 (n=155), ceBG35 (n=516), ceBG37 (n=1012), ceBG40 (n=176), ceBG459 (n=1441), ceBG621 (n=787), ceBG1272 (n=586). The ancient sample was not included in ceBG1272 in both (A) and (B).
Extended Data Fig. 4	The geographic states of the ancestral nodes in the Choleraesuis population after downsamplings.	Extended_Data_Fig_4 .eps	(A) Downsampling tests of up to ten strains per country/region. (B) Downsampling tests of up to five strains per country/region. Both: the geographic states were predicted using TreeTime. Each test was run in 100 parallels. The pie charts illustrate the proportions of the best-supported geographic states in the 100 parallels for the corresponding ancestral nodes.
Extended Data Fig. 5	Reconstructed ancestral host associations for all nodes in nine pig-enriched ceBGs	Extended_Data_Fig_5 .eps	The corresponding ceBGs for each panel are: (A) ceBG3 (Derby), (B) ceBG1272 (Choleraesuis), (C) ceBG17 (Chailey), (D) ceBG35 (Worthington), (E) ceBG37 (London), (F) ceBG40 (Cerro), (G) ceBG459 (Johannesburg), (H) ceBG621 (Ohio), (I) ceBG10 (Adelaide). The mean values of effective population sizes with time were also shown for (A) and (B), with 95% confidence intervals in grey shapes. The orange and grey boxes show the periods of population expansion (A, B) or the periods of host transfers into pigs (C-I).
Extended Data Fig. 6	The host transmission frequency of nine pig-enriched ceBGs.	Extended_Data_Fig_6 .eps	The corresponding ceBGs for each panel are: (A) ceBG10 (Adelaide), (B) ceBG1272 (Choleraesuis), (C) ceBG17 (Chailey), (D) ceBG3 (Derby), (E) ceBG35 (Worthington), (F) ceBG37 (London), (G) ceBG 40 (Cerro), (H) ceBG 459 (Johannesburg),

			(I) ceBG 621 (Ohio). Different arrows represent the direction of host transmission, with darker colors indicating higher transfer frequency. “*” marks the most contributing host sources for the transmissions.
Extended Data Fig. 7	A 5 X 5 table showing the summarised international transmission events of all nine pig-enriched ceBGs in <i>Salmonella</i> in the past 50 years.	Extended_Data_Fig_7 .eps	The maximum-likelihood phylogeny was reconstructed based on SNPs in the core genome of each ceBG and the date of origin was estimated using BactDating. TreeTime was applied to reconstruct the country sources for all nodes in the tree. A transmission was recorded when the ancestral node and descending node of a branch were different. All transmissions were then summarized and grouped based on their associated continents.
Extended Data Fig. 8	Pearson’s correlations analysis of sub-classification for pig-related products.	Extended_Data_Fig_8 .eps	The Sub classifications involved include (A) Pork offal, frozen (021011); (B) Pork, frozen (020649); (C) Pork, frozen cut (020329); (D) Pork, preserved (020322); (E) Pork offal, fresh (020630); (F) Pig fat (020910); (G) Pork, fresh cuted (020912); (H) Pork, fresh (020319); (I) Pig carcasses (020310); (J) Pig, live breeding (010391); (K) Pig, live, less 50kg (010392); (L) Pig, live, over 50kg (020311). The codes in parentheses represent the Harmonized System Codes of the products. Analyzing the correlation between the intercontinental dissemination of each pig-related commodity and the intercontinental transmission of pig-enriched ceBGs. R: Pearson’s correlation coefficient.

14

15 **1. Supplementary Information:**

16 **A. PDF Files**

Item	Present?	Filename	A brief, numerical description of file contents.
		Whole original file name including extension. i. e. : Smith_SI.pdf. The extension must be .pdf	<i>i. e. : Supplementary Figures 1-4, Supplementary Discussion, and Supplementary Tables 1-4.</i>

Supplementary Information	Yes	Supplementary_Information.pdf	Supplementary Tables 1-4.
Reporting Summary	Yes	6823_1_attach_25_30962.pdf	

17

18

19

B. Additional Supplementary Files

Type	Number Each type of file (Table, Video, etc.) should be numbered from 1 onwards. Multiple files of the same type should be listed in sequence, i.e.: Supplementary Video 1, Supplementary Video 2, etc.	Filename Whole original file name including extension. i.e.: <i>Smith_Supplementary_Video_1.mov</i>	Legend or Descriptive Caption Describe the contents of the file
Supplementary Table	Additional Supplementary Files Table 1	Additional_Supplementary_Files.xlsx	In the manuscript and Additional Supplementary Files Table 1
Supplementary Table	Additional Supplementary Files Table 2	Additional_Supplementary_Files.xlsx	In the manuscript and Additional Supplementary Files Table 2

20

21

22 **3. Source Data**

Parent Figure or Table	Filename Whole original file name including extension. i.e.: <i>Smith_SourceData_Fig1.xls</i> , or <i>Smith_Unmodified_Gels_Fig1.pdf</i>	Data description i.e.: Unprocessed western Blots and/or gels, Statistical Source Data, etc.
Source Data Fig. 1	SourceData_Figure_1.xlsx	Statistical Source Data
Source Data Fig. 2	SourceData_Figure_2.xlsx; SourceData_Figure_2D_and_2F.txt; SourceData_Figure_2F.txt	Statistical Source Data
Source Data Fig. 3	SourceData_Figure_3A_and_ExtendedData_Figure_5.zip; SourceData_Figure3_and_ExtendedData_Figure6.xlsx	Statistical Source Data
Source Data Fig. 4	SourceData_Figure4BC_and_ExtendedData_Fig7.xlsx; SourceData_Figure4A_and_4DEFG_ExtendedData_Figure_8.xlsx	Statistical Source Data
Source Data Extended Data Fig./Table 1	SourceData_ExtendedData_Figure1.txt	Statistical Source Data
Source Data Extended Data Fig./Table 2	SourceData_ExtendedData_Figure2_and_Figure4.xlsx	Statistical Source Data

Source Data Extended Data Fig./Table 3	SourceData_ExtendedData_Figure3.xlsx	Statistical Source Data
Source Data Extended Data Fig./Table 4	SourceData_ExtendedData_Figure2_and_Figure4.xlsx	Statistical Source Data
Source Data Extended Data Fig./Table 5	SourceData_Figure3A_and_ExtendedData_Figure5.zip	Statistical Source Data
Source Data Extended Data Fig./Table 6	SourceData_Figure3_and_ExtendedData_Figure6.xlsx	Statistical Source Data
Source Data Extended Data Fig./Table 7	SourceData_Figure4BC_and_ExtendedData_Figure7.xlsx	Statistical Source Data
Source Data Extended Data Fig./Table 8	SourceData_Figure4A_4DEFG_and_ExtendedData_Figure8.xlsx	Statistical Source Data

25 **Centralized industrialization of pork in Europe and America contributes to**
26 **the global spread of *Salmonella enterica***

27 Heng Li ^{1,2}, Yilei Wu ^{1,3}, Dan Feng ^{1,2}, Quanguai Jiang ^{1,2}, Shengkai Li ¹, Jie Rong ¹, Ling Zhong
28 ¹, Ulrich Methner ⁴, Laura Baxter ⁵, Sascha Ott ⁶, Daniel Falush⁷, Zhenpeng Li⁸, Xiangyu Deng⁹,
29 Xin Lu ⁸, Yi Ren ¹⁰, Biao Kan ⁸, Zhemin Zhou ^{1,2,8*}

30 **Affiliations**

31 ¹ Key Laboratory of Alkene-carbon Fibres-based Technology & Application for Detection of
32 Major Infectious Diseases, MOE Key Laboratory of Geriatric Diseases and Immunology,
33 Pasteurien College, Suzhou Medical College, Soochow University, Suzhou, China

34 ² Suzhou Key Laboratory of Pathogen Bioscience and Anti-infective Medicine, Jiangsu Province
35 Engineering Research Center of Precision Diagnostics and Therapeutics Development, Soochow
36 University, Suzhou, China

37 ³ Department of Biological Sciences, Xi'an Jiaotong-Liverpool University, Suzhou, China

38 ⁴ Institute of Bacterial Infections and Zoonoses, Friedrich-Loeffler-Institut, Jena, Germany

39 ⁵ Warwick Bioinformatics Research Technology Platform, University of Warwick, Coventry,
40 UK

41 ⁶ Warwick Medical School, University of Warwick, Coventry, UK

42 ⁷ The Center for Microbes, Development and Health, CAS Key Laboratory of Molecular
43 Virology and Immunology, Shanghai Institute of Immunity and Infection, Chinese Academy of
44 Sciences, Shanghai, China

45 ⁸ National Key Laboratory of Intelligent Tracking and Forecasting for Infectious Diseases,
46 National Institute for Communicable Disease Control and Prevention, Chinese Center for
47 Disease Control and Prevention, Beijing, China

48 ⁹ Center for Food Safety, University of Georgia, Griffin GA, USA

49 ¹⁰ Iotabiome Biotechnology Inc., Suzhou, China

50

51 **Abstract**

52 *Salmonella enterica* (*S. enterica*) causes severe foodborne infections through contamination of
53 the food supply chain. Its evolution has been associated with human activities, especially animal
54 husbandry. Advances in intensive farming and global transportation have substantially reshaped
55 the pig industry, but their impact on the evolution of associated zoonotic pathogens such as *S.*
56 *enterica* remains unresolved. Here we investigated the population fluctuation, accumulation of
57 antimicrobial-resistant genes, and international serovar Choleraesuis transmission of nine pig-
58 enriched *S. enterica* populations comprising more than 9000 genomes. Most changes were found
59 to be attributable to the developments of the modern pig industry. All pig-enriched salmonellae
60 experienced host transfers in pigs and/or population expansions over the past century, with pigs
61 and pork having become the main sources of *S. enterica* transmissions to other hosts. Overall,
62 our analysis revealed strong associations between the transmission of pig-enriched salmonellae
63 and the global pork trade.

64

65

66 **Main**

67 *Salmonella enterica* infiltrates food supply chains through the contamination of food, water, or
68 food-processing facilities¹, resulting in life-threatening foodborne infections with 108.1 million
69 illnesses and 291,000 deaths annually². Pork and pigs are prominent sources of *S. enterica*
70 infections, accounting for ~31.1% of salmonellosis and 9.3% of disease outbreaks in the
71 European Union³. Despite its acknowledged role in mediating transmissions and outbreaks of
72 viral diseases^{4,5}, the contribution of pigs to the global dissemination of bacterial pathogens,
73 including *S. enterica*, remains insufficiently explored within the framework of the “One Health”
74 strategy.

75 The developments of intensive farming and global trade over the past century have drastically
76 transformed pig agriculture⁶, giving rise to two industrial hubs, Europe and the US, that
77 collectively represent >32% of international pork and pig breed trades^{7,8}. While most of
78 the >2000 populations in *S. enterica*, recognized by their serovars, eBGs, or ceBGs based on the
79 genomic sequences⁹, are ubiquitous, some populations predominantly comprise strains
80 associated with pigs¹⁰ and are found to spread regionally through movements of pigs and/or wild
81 boars¹¹. Nonetheless, it remains unclear how pathogens, especially these pig-enriched
82 salmonellae, have disseminated globally and how their population dynamics have been recrafted
83 by modern agriculture.

84 **Results**

85 **Landscape of pig-enriched *Salmonella enterica* populations**

86 Systematic investigation of all 362,931 *Salmonella* strains publicly accessible in EnteroBase
87 (July 2022) showed that pigs/pork accounts for 17,623 strains (4.9%) in 252 ceBGs and is the 2nd
88 most frequent livestock source of *S. enterica* after poultry over the past century (Fig. 1A, B).
89 There are 61 major ceBGs that each contains ≥ 20 pig-related strains, of which nine have $\geq 40\%$
90 of their strains from pigs/pork (Fig. 1C, D; Additional Supplementary Files Table 1), including
91 prominent pig-enriched populations such as ceBG1272 (Choleraesuis) and ceBG3 (Derby), and
92 others like ceBG10 (Adelaide) and ceBG459 (Johannesburg). Pig is the primary source (4393;
93 49%) of strains in these 9 pig-enriched ceBGs, followed by humans (2482; 28%) and other

94 animals (1279; 14%). The other ceBGs have lower levels of pig-associated strains (0.2-38%)
95 and exhibit no clear host preference, including ceBG2 (Typhimurium) which has only 6% (4612)
96 of pig-associated strains (Fig. 1C, D).

97 The HC5 clusters in EnteroBase, namely clusters of strains with ≤ 5 allelic differences in their
98 core genes, have been extensively used in epidemiological investigations for designating
99 genetically almost identical bacteria such as those from disease outbreaks¹². Unexpectedly, while
100 most HC5s in the pig-enriched ceBGs are from single countries, there are 35 HC5s each
101 consisting of strains from ≥ 2 countries, including 15 HC5s with strains from different continents
102 (Supplementary Table S1), indicating very recent international or even cross-continental
103 transmissions. Notably, all these international HC5s contain at least one pig strain, prompting the
104 importance of pigs for these long-range transmissions.

105

106 **Europe as the main genetic repository of serovar Choleraesuis**

107 We reconstructed a maximum-likelihood phylogeny of serovar Choleraesuis based on 21,948 non-
108 repetitive, non-recombinant single nucleotide polymorphisms (SNPs) in the core genome and used it
109 to divide strains into three lineages of CS1, CS2, and CS3 from the root that were separated by 2932
110 to 12,435 SNPs (Additional Supplementary Files Table 2). Except for CS3 which contained only two
111 strains, the other two lineages were subdivided into clades and clusters (Fig. 2A and Extended Data
112 Fig. 1). CS1 consists of 8 clusters in two clades of CS1.1 and CS1.2, and CS2 consists of 19 clusters
113 in three clades of CS2.1 to CS2.3. High geographic and host specificities were found in certain clades
114 and clusters. For example, most of the strains in Chinese mainland and Vietnam fell into Clade 1.2,
115 while many of the British strains were from Clade 1.1. In addition, 92% of the US strains grouped
116 with those from Chinese Taiwan in Clade 2.2, while >60% of European wild boar strains were from
117 Clades 2.3.

118 We evaluated the genetic diversity of Choleraesuis in different regions worldwide. The Simpson's
119 diversity index (SDI) for the presence of clades in different regions (Fig. 2E) showed that West
120 and North European regions had the greatest levels of diversities (0.66 – 0.7), followed by South
121 America and East Asia (0.63). In contrast, Africa and North America had the lowest SDIs (0.14

122 and 0.17, respectively). Furthermore, to minimize the impact of oversampling in developed
123 countries, we performed a country-level comparison, which also showed that the countries from
124 North Europe exhibited greater levels of SDIs than those from other regions (Supplementary Table
125 S2). This suggested Europe as the main genetic repository and probably the origin of serovar
126 Choleraesuis (Fig. 2E).

127

128 **Host-specific ARGs accumulation in Choleraesuis**

129 Choleraesuis strains carried many more antimicrobial resistant genes (ARGs) than its human-
130 specific analog, Paratyphi C (Fig. 2B, C), which was separated from serovar Choleraesuis only
131 ~4000yrs ago, suggesting an association between hosts and ARGs. Furthermore, significant
132 differences in ARG levels were found between Choleraesuis strains from different hosts and
133 countries/regions. In particular, strains from humans and livestock carried ~9-fold more ARGs
134 than those from wild boars (Fig. 2C), and strains from Chinese Taiwan and Vietnam carried more
135 ARGs than those from others (Fig. 2D).

136 Moreover, Choleraesuis isolated from pigs exhibited high resistance against aminoglycoside,
137 sulfonamide, tetracycline, and beta-lactam, which were all common feed supplements for
138 intensive farming¹² (Fig. 2A). In contrast, resistances against clinical antimicrobials including
139 quinolone, trimethoprim, and cephalosporins were much fewer, and often found only in human
140 strains. Notably, the colistin-resistant genes, *mcr-1* and *mcr-3*, commonly detected in pigs¹³, were
141 found in eight human/pig strains from the UK, China, Brazil, and Germany, underscoring their
142 global presence (Supplementary Table S3). Additionally, continuous increases in ARG carriages
143 over time were spotted in CS1 and CS2 strains isolated after the 1970s (Fig. 2B), except that the
144 ARG carriages in CS2 dropped after the 2010s due to an increase of strains from wild boars.

145

146 **International transmission of serovar Choleraesuis**

147 Significant temporal signals were detected in serovar Choleraesuis, with and without the ancient
148 genotype (Extended Data Figs. 2 and 3). Bayesian inferences predicted that the most recent

149 common ancestor (MRCA) of *Choleraesuis* had probably been circulating in Europe before 2394
150 BP (CI95% 2276-2521 BP) and diverged there into CS1 and CS2 in 1785 and 1870, respectively
151 (Fig. 2F). The first predicted transmission outside of Europe occurred before 1893 (CI95% 1891-
152 1896) and resulted in Clade CS2.2 in the US. Soon after, the effective population size of
153 *Choleraesuis* was predicted to experience an expansion in the early 20th, coincident with the rapid
154 development of intensive pig farming, and reached its first peak in the 1930s, before the
155 commercial use of synthetic sulphonamides and other antimicrobials in animals¹⁴.

156 After 20 years of stale, a second expansion of *Choleraesuis* was predicted between the 1950s and
157 the 1980s (Fig. 2G). The frequencies of international transmissions also increased, possibly
158 associated with the rapid expansion of global agricultural trade as part of the post-war waves of
159 livestock revolution and trade globalization¹⁵. Europe and the US were the major sources of
160 international transmissions. For example, European CS1 strains were repetitively transmitted to
161 Chinese mainland and Southeast Asia (Fig. 2F). Furthermore, CS2.2 strains were transmitted from
162 the US to Chinese Taiwan (Fig. 2F, CS2.2.4) in 1962 (CI95% 1957-1968) and became endemic
163 there for more than 50 years, causing major human outbreaks between 1996 and 2002¹⁶. The
164 population size of *Choleraesuis* reached its peak in 1985 and underwent continuous decreases
165 afterward (Fig. 2G). This was also accompanied by a decrease in long-range transmissions,
166 although the local transmissions in Europe remained frequent, partially attributed to the movement
167 of wild boars¹⁷.

168 The majority of the *Choleraesuis* genomes were isolated from North European countries, which
169 could lead to sampling bias in the analyses. Therefore, we performed phylogeographic
170 reconstructions by downsampling at most ten random genomes from each country (Extended Data
171 Fig. 4 and Supplementary Table S4). Summarising 100 downsampling results together, we found
172 that the MRCA of *Choleraesuis*, as well as the MRCAs of all major clades except for Clade 2.1,
173 were still from North Europe (Extended Data Fig. 4A). Downsampling to at most five genomes
174 per country still proposed North Europe as the origin of the whole population but made Peru the
175 origin of Lineage 1 (Extended Data Fig. 4B). These differences likely resulted from the fact that
176 there was only one cluster of strains for each of Peru and Cameroon near the basal of Clade 2.1
177 and Lineage 1, respectively.

178

179 **Intensive farming in establishments of pig-enriched serovars**

180 We further evaluated the role of pigs in the evolution of all nine pig-enriched populations. To this
181 end, we demonstrated the presence of temporal signals in all nine populations by date
182 randomisations (Extended Data Fig. 3) and estimated their temporal phylogenies and ancestral
183 host transfers. Notably, apart from ceBG40 (Cerro) which originated around 1954, the MRCA for
184 other populations were all predicted to be present before the 19th century (Fig. 3A and Extended
185 Data Fig. 5). However, except for ceBG3 (Derby) and ceBG1272 (Choleraesuis), other
186 populations were originally present in hosts other than pigs, and only transferred into pigs after
187 1930. Furthermore, we evidenced at least eight human-to-pig transmissions in ceBG3 (Derby)
188 during 1906-1942, resulting in the establishment of the contemporary pig-enriched lineages and
189 major population expansion (Extended Data Fig. 5A). Thus, all pig-associated salmonellae, apart
190 from Choleraesuis, likely experienced host transfers in the 20th century (Fig. 3A). Furthermore, the
191 accumulation of pseudogenes has been associated with a drastic change, such as host adaptation of
192 the bacteria. However, we did not evidence an accumulation of pseudogenes in any population (Fig.
193 3D), except for the pig-adapted Choleraesuis which has >17.3% of its genes disrupted⁷.

194 Different from the long-term trend of human-to-pig transfers, the majority (30-60%) of the recent
195 host transfers in these populations, including those into humans, have been contributed by pigs in
196 the past 50 years (Fig. 3B and Extended Data Fig. 6). Conversely, pigs contribute much less to host
197 transfers in eight populations that had lower proportions (7-38%) of pig strains (Fig. 3C),
198 demonstrating the importance of pigs from intensive farming as a hub of host transfers in the pig-
199 enriched populations.

200

201 **Dispersal of *Salmonella enterica* from Europe and America**

202 The reconstructed international transmissions in all nine populations showed that 68-96% of
203 transmissions into each continent were from either Europe or America (Fig. 4A), exhibiting
204 similar patterns to the trade data of the pork-related products in the Harvard database (Fig. 4B).
205 We then summarized the cross-continental trades for each of the 5,014 product categories in the

206 Harvard database. The transmission of pig-enriched salmonellae was shown in a 5×5 table, in
207 which rows and columns represented the continental sources and targets, and each cell showed the
208 percentage contribution of a source continent to the influx of the target (Extended Data Fig. 7).
209 This resulted in a dataset for trade/transmissions, of which the pairwise Pearson's correlations
210 were calculated and projected to a 2-D space using an unsupervised method, the uniform manifold
211 approximation and projection (UMAP)¹⁸ (Fig. 4C).

212 The trade data for most of the animal-related products fell into two clusters in the projection. The
213 first cluster consisted of almost all bovine and poultry products as well as live pigs, and the second
214 cluster consisted of five pig-related products and one poultry product. Impressively, the
215 transmission of the pig-enriched salmonellae also fell in the second cluster, exhibiting 0.87-0.96
216 correlation coefficients to the pig-related products ($p < 0.0001$) (Fig. 4C). Detailed investigation of
217 the products in the 2nd cluster suggested that they were either frozen or processed pork or offal and
218 fat that could be transported over long distances and used for pig feeding¹⁹. Pig-enriched
219 salmonellae exhibited greater correlation with these products than that of fresh pork and live pigs
220 (Fig. 4D-G), which also correlated to pathogen transmissions with lower, yet significant
221 coefficients of 0.46-0.72 (Fig. 5 and Extended Data Fig. 8).

222

223 **Discussion**

224 The modern agriculture system, including intensive farming and global transportation, has
225 significantly recrafted the daily life of not only livestock animals but also ourselves⁶. But how
226 much has it modified the life of bacteria, particularly, the zoonotic pathogens? Here based on
227 genomic analysis of >9000 pig-associated strains, we demonstrated that the modernization and
228 globalization of agriculture in the past century had driven the emergences, population expansions,
229 ARG acquisitions, and global transmissions of pig-enriched salmonellae.

230 We initiated the investigation in *Choleraesuis*, a prominent serovar that has been specifically
231 infecting both pigs and humans for >2000 years¹¹. Compared to previous studies that focused on
232 either its ancient divergence or regional dissemination¹¹, we compiled a global dataset of
233 *Choleraesuis* strains to give a comprehensive overview of its recent evolution. We demonstrated

234 the high occurrences of cross-continental transmissions with a peak in the 1950s-1980s, a period
235 of accelerated globalization before the use of specific vaccines²⁰. The most obvious example is
236 between the Chinese mainland and Taiwan. Despite their geographic closeness, almost all strains
237 in the Chinese mainland were in Clade 1.2 and imported from Europe, whereas strains in Chinese
238 Taiwan were in Cluster 2.2.4 and imported from the US. We attributed this to the different trading
239 partners between the two regions. The Chinese mainland mostly imported pork and pig breeds
240 such as Yorkshires and Landraces from Europe during 1950-2000²¹, whilst Chinese Taiwan traded
241 more frequently with the US²².

242 The quinolone-resistant *Salmonella* has been regarded as an “Urgent threat” and is widely found
243 in Typhi and Paratyphi A²³. We found that 38% and 10.8% of Choleraesuis strains from humans
244 and pigs were also quinolone-resistant, mediated by either mutation in QRDR (quinolone
245 resistance-determining regions) or acquisition of ARGs (Additional Supplementary Files Table 2).
246 Furthermore, many quinolone-resistant strains, especially the human strains in Clusters 1.1.1,
247 1.2.1, and 2.2.4, also exhibit resistance to many antimicrobials extensively used in animals and
248 clinical settings and expose imminent threats to public health. For example, the strains from
249 Cluster 2.2.4 have been epidemic in Chinese Taiwan during 1995-2003¹⁶. Particularly, compared
250 to those from wild boar, strains from pigs and humans had 10× more ARGs or QRDR mutations,
251 revealing a strong association between the extensive animal use of antimicrobials and the
252 emergence of extensive-resistant pathogens²⁴ and demonstrating the importance of the “One
253 Health” strategy in the control of antimicrobial overuse.

254 Nine pig-enriched *Salmonella* populations were identified from the ~362K genomes in
255 EnteroBase. Some Typhimurium clades were previously reported as pig-adapted based on small,
256 local datasets²⁵, but not in our survey of >70K genomes (Fig. 1C). In contrast, we showed that two
257 prominent pig-associated serovars, ceBG1272 (Choleraesuis) and ceBG3 (Derby), have been
258 associated with pigs for millennia^{26,27} and experienced significant population expansions after the
259 1900s. Besides, the other seven pig-enriched populations were not associated with pigs until the
260 1900s, during which they all experienced host jumps into pigs. We noticed the development of
261 intensive pig farming during the beginning of the 1900s, which could increase the pig-pig contacts
262 while reducing those between pigs and humans. Such an environment could increase the chance of
263 transmission among the pig populations while reducing spillover between the hosts, facilitating the

264 establishment of host-enriched pathogens. Similar host transfer and population expansion have
265 been observed in *Mycobacterium tuberculosis*, which was associated with increased contact
266 between humans after the invention of fire use²⁸. Thus, we attributed the increased host jumps and
267 population expansion of salmonellae in the pig population to the development of intensive pig
268 farming in the 20th century, which is in need of further research.

269 We showed that the vast majority of the contemporary non-human strains from these nine
270 populations were from pig/pork, and proved that pig is the primary source of their host transfer
271 events (Fig. 3B). The chance that strains from these nine pig-enriched populations being
272 transmitted by other non-human hosts, while could still occur, is low. Thus, we hypothesized that
273 pig-related routes, including pork and pigs, the major sources of *S. enterica* infections²⁹ were the
274 dominant ways for the transmission of these *salmonellae*. International salmonellosis outbreaks
275 due to global transportation of end products have been extensively reported, such as those by
276 hams³⁰ or chocolates³¹. However, most of these events resulted in infections in humans, which
277 represents a sink of the pathogen and rarely mediated population expansion or secondary
278 transmissions into animals³². In contrast, transmissions via poultry breeding stocks³³ or animal
279 feeds³⁰ could lead to long-term epidemics or permanent establishment of the bacteria in the target
280 regions. Furthermore, transmission of pig pathogens has been more frequently associated with the
281 end products due to the common application of swill feeding¹⁹, as evidenced in foot-and-mouth
282 disease virus (FMDV) outbreaks⁴, African swine fever virus (ASFV)⁵, and trichinosis³⁴. Based on
283 the UMAP analysis, we revealed strong associations between the global pork trade and the
284 transmissions of pig-enriched salmonellae. This indicated that the predominance of modern pig
285 industries in Europe and the Americas made them the centers of development and global
286 dissemination of salmonellae, highlighting the role of agricultural practice as a driver of the
287 geographic dispersal of associated bacterial pathogens.

288 A limitation of this work is that the majority of involved genomes were from public databases and
289 had sampling bias towards developed countries. The genetic diversities of pig-enriched
290 salmonellae in the majority of developing countries, especially those in South America and Africa
291 have not been sampled. Downsampling was adopted to reduce the influence of such bias, but, as
292 evidenced in *Choleraesuis*, itself could introduce a bias towards countries of low genetic

293 diversities. Furthermore, there is not enough data for investigation of local transmissions driven by
294 country-wide agricultural transportation or the movements of wild boars, as previously reported ³⁵.

295 In summary, our findings demonstrate the influence of modern agriculture on the population
296 dynamics of *S. enterica*. The intensive farming has driven the host jumps of many *S. enterica*
297 populations into pigs and population expansion of the pig-associated populations, the widespread
298 availability of antibiotics after the 1940s increased the prevalence of antimicrobial resistance
299 (AMR), and the expansion of globalized trade and transportation resulted in rapid and frequent
300 global dissemination of these pig-enriched *S. enterica* (Fig. 5). Despite decades of significant
301 progress on *Salmonella* control in pigs, the evidence provided here warrants further investigation
302 and potential intervention into the global spread of *S. enterica* from centralized origins at the
303 pinnacle of pork production.

304

305 **Methods**

306 **Strains and whole-genome sequencing procedures**

307 The metadata associated with all 362,931 *S. enterica* strains accessible in EnteroBase (July 2022)
308 was downloaded and manually classified into seven categories: Pig, Bovine, Poultry, Human, other
309 Animals, and Food/Environment. The serovar associated with each ceBG (HC900 cluster) was
310 downloaded from https://enterobase.readthedocs.io/en/latest/HierCC_lookup.html. A subset of 61
311 ceBGs with ≥ 20 pig strains (277,588 strains in total) was used to display as a hierarchical bubble
312 plot (Fig. 1D), showing phylogenetic grouping at subspecies (HC2850), super-lineage (HC2000), and
313 ceBG (HC900) levels, along with pie charts representing source category. A total of 9,259 genomes
314 from 9 ceBGs each containing $>40\%$ of pig-associated strains were selected for downstream
315 analysis. Additionally, a set of 16,829 genomes from 8 pig-containing ceBGs that each contain
316 lower levels (2-40%) of pig-associated strains were also selected in comparison with the 9 pig-
317 enriched ceBGs. Additionally, 15 *Choleraesuis* strains were collected by China CDC from northern
318 and eastern regions across China between 2002 and 2022. The DNA of each strain was extracted
319 using the HiPure Bacterial DNA kit (D3146). Paired-end libraries with insert sizes of ~ 300 bp were
320 prepared following Illumina's standard genomic DNA library preparation procedure (VAHTS

321 Universal DNA Library Prep kit for Illumina V3) and sequenced on an Illumina NovaSeq 6000
322 using the S4 reagent kits (v1.5) according to the manufacturer's instructions.

323 To demonstrate the association between pig and its enriched *S. enterica* strains, we sequenced the
324 genome of 78 strains of the prominent pig-enriched serovar, Choleraesuis. These include 63
325 strains from Germany or Austria as part of the University of Warwick/University College Cork
326 10K genomes project³⁶ and 15 from China. They were integrated with public genomes of 679
327 strains isolated between 1935 and 2022 and one genotype reconstructed from a ~1600-year-old
328 human remains³⁷, resulting in a global collection of 757 genomes (Additional Supplementary Files
329 Table 2) encompassing 41 countries.

330

331 **Bioinformatic analysis**

332 The sequencing reads of each strain were quality trimmed using EtoKi prepare¹², and the high-
333 quality sequences were further assembled into contigs using SPAdes V3.13³⁸ which was
334 implemented in the 'EtoKi assemble' pipeline. The genes in each assembled genome were predicted
335 and annotated using PROKKA 1.14.6³⁹ and had detailed functional predictions using eggno-
336 mapper v2⁴⁰. The antibiotic resistance genes were predicted using AMRfinder v3.11.14⁴¹, and the
337 disrupted genes in the pig-enriched populations were predicted using PEPPAN⁴². The multi-
338 sequence alignment for each pig-enriched ceBG was generated using the EtoKi align module and
339 used to build a maximum-likelihood (ML) phylogeny using IQTree v1.6.12⁴³ implemented in EtoKi
340 phylo after the removal of recombinant regions using RecHMM¹¹.

341

342 **Temporal signal and randomization test**

343 The presence of a temporal signal in *Salmonella* serovar Choleraesuis (ceBG1272) was tested using
344 three approaches. The regression of root-to-tip distances and dates of isolation was estimated using
345 TempEst v1.5.3⁴⁴ with a correlation of determination (R^2) of 0.67 and P-value of 4.15×10^{-6} . We
346 then randomly permuted the isolation dates of the strains ten times and estimated their R^2 values.
347 The same datasets were also used for BactDating v1.1⁴⁵ inferences as described above, and their
348 substitution rates were compared with the rate from the actual data (Extended Data Fig. 2),

349 demonstrating the presence of a significant temporal signal. We also performed the same tests
350 without the ancient genotype, demonstrating the presence of temporal signals. Furthermore, the
351 tests were also performed for the other eight pig-enriched populations, proving their availability for
352 temporal analyses (Extended Data Fig. 3).

353

354 **Population dynamics of serovar Choleraesuis**

355 The ML tree of serovar Choleraesuis was calibrated by dated tips using BEAST⁴⁴ with a GTR
356 substitution model and fixed topology. Eight BEAST runs were prepared by combinations of two
357 clock models of “strict clock rate” and “optimised relaxed clock”, and four population models of
358 “constant coalescence”, “Bayesian skyline”, “Birth-death skyline” and “extended Bayesian
359 skyline”. All models were run in “Nested Sampling” mode with 8 parallel chains each with
360 “chainLength=20000”, “particleCount=1”, and “subChainLength=5000”. The results were
361 summarized using NSLogAnalyser and the model with “optimised relaxed clock” and “Bayesian
362 skyline” had the greatest marginal likelihood with a maximum ESS of 632.3. The posterior trees
363 from the best model were then summarized using treeannotator into a maximum clade credibility
364 tree (MCC tree) and visualized in iTol⁴⁶.

365 Two downsampling tests were performed by selecting at most ten or five random genomes from
366 each country. We employed TreeTime to reconstruct the ancestral states of the internal nodes based
367 on a subtree containing only those selected tips. Each test was run parallel 100 times, and the results
368 were summarized in Extended Data Fig. 4.

369

370 **Population dynamics of pig-enriched and pig-containing ceBGs**

371 Furthermore, the population dynamics of each pig-enriched population were estimated using
372 BactDating⁴⁷, which performed Bayesian inference of ancestral dates based on the ML tree. Parallel
373 chains of 5e6 samples each were run for each of the substitution models of “strictgamma”,
374 “mixedgamma”, and “carc”. The first 50% of the chain (3e6 samples) for each model was discarded
375 as burn-ins and the convergence of the run was determined by ensuring effective sampling sizes
376 (ESSs) of >100 for all parameters. The results from all samples were compared based on their
377 Bayes Factors using the modelcompare function in BactDating, and only the best model for each

378 pig-enriched population was reported. Notably, the dating results for ceBG1272 (Choleraesuis) by
379 BactDating were very similar to that by BEAST, suggesting high reproducibility of the analyses.
380 We then estimated the host transfers and geographic transmissions of each population along the
381 dated trees using the ML algorithm implemented in TreeTime⁴⁸. Similarly, the dates and host
382 transfers of the ancestral nodes in the ML trees of the pig-containing ceBGs were also estimated as
383 described above.

384

385 **Transmission events and the correlation between trade data**

386 We define a transmission or host transfer event when the ancestral node and the descending node
387 of a branch are assigned different country/host information. Considering all possible states as S .
388 A host transfer or international transmission was counted along the ML tree if the reconstructed
389 states in the ancestral and the descending nodes of a branch were different, and the numbers of
390 host transfers and international transmissions were summarized as $N_{i \rightarrow j}$, where $i \in S$ and $j \in S$ are
391 the states of the ancestral and descending nodes, respectively. Then there is:

$$392 \quad T_{i \rightarrow j} = N_{i \rightarrow j} / \sum_{k \in S} N_{k \rightarrow j}$$

393 Where $T_{i \rightarrow j}$ is the normalized frequency of S_j originating from S_i , and $k \in S$ is an iterator for
394 calculating the total number of transmissions into S_j . Furthermore, the normalized frequency
395 between two continents m and n are:

$$396 \quad \hat{T}_{m \rightarrow n} = \sum_{a \in m} \sum_{b \in n} T_{a \rightarrow b}$$

397 Where a and b are countries in the continents m and n , respectively.

398

399 The international trade data of all categories were obtained from Harvard Dataverse
400 (<https://dataverse.harvard.edu>). Trade values were expressed in constant U.S. dollars after
401 adjustment for inflation and summed up. The normalized fluxes of trade between continents were
402 also calculated using a procedure similar to the above. As a result, frequencies of pathogen
403 transmissions and trading among five continents of Asia, Africa, Europe, Oceania, and the

404 Americas were obtained and pairwise Pearson's correlation coefficients (R) between the cross-
405 continental flows of the goods and between the flows of the goods and the pathogens were
406 calculated. All goods and salmonellae were then projected into a 2-D space based on their I - R
407 values using UMAP (Uniform Manifold Approximation and Projection), which is a non-linear
408 dimension reduction technique that has been extensively used in biological analysis, such as in
409 single-cell studies⁴⁹.

410

411 **Data availability**

412 The raw sequencing reads for the 15 Chinese strains have been deposited in the Genome Sequence
413 Archive in the National Genomics Data Center, China National Center for Bioinformation / Beijing
414 Institute of Genomics, Chinese Academy of Sciences (GSA: CRA012579) and are publicly
415 accessible at <https://ngdc.cnbc.ac.cn/gsa>. The assembled genome sequences have been deposited in
416 the Genome Warehouse (GWH) in the National Genomics Data Center with BioProject accession
417 PRJCA019682. The raw reads for 67 European Choleraesuis strains were deposited in Short Reads
418 Archive (SRA) at EBI under BioProject accession: PRJEB20997, as part of the University of
419 Warwick/University College Cork (UOWUCC) 10K genomes project. A detailed list of the sample
420 accession codes for all Choleraesuis strains is available in Additional Supplementary Files Table 2.
421 Assembled genomes for all pig-enriched populations were available as a workspace in EnteroBase
422 at <https://enterobase.warwick.ac.uk/a/100355>. The resulting figures and underlying data of 61
423 ceBGs with ≥ 20 pig strains are all available at <https://observablehq.com/d/232a986be1a99113>.

424 **Acknowledgments**

425 HL, YW, DFeng, QJ, and SL contributed equally to this work. The project was supported by the
426 National Natural Science Foundation of China (No. 32170003 (ZZ), No. 32370099 (ZZ), No.
427 82202465 (HL)), the Major Projects of the National Natural Science Foundation of China
428 (22193064 (BK and XL)), the Natural Science Foundation of Jiangsu Province (BK20211311
429 (ZZ)), and the Suzhou Science and Technology Innovations Project in Health Care (SKY2021013
430 (ZZ)).

431 **Competing interests**

432 The authors declare no conflicts of interest.

433 **Authors' contributions**

434 HL, YR, XL, ZZ designed the study. UM, XL applied the experiments, DFeng, QJ, JR, and LB
435 prepared the figures and tables. LZ, SL, YR, ZL analysed the statistical data. HL, YW, DFeng, ZZ
436 wrote the initial version of the manuscript. HL, DFeng, SO, DFalush, XD, BK, ZZ revised the
437 manuscript.

438

439

440 **Figure Legends**

441 **Fig. 1 | Summary of the pig-enriched ceBGs in the *Salmonella* database in EnteroBase. (A)**

442 Histogram of the numbers of *Salmonella* strains for each non-human source in EnteroBase. (B)

443 Histogram of the numbers of pig-associated *Salmonella* strains per year during 1885-2022. (C) Bubble

444 plot of the 61 pig-associated ceBGs each with ≥ 20 strains. Each ceBG is sized proportional to the

445 number of strains in it, and placed according to the numbers and percentages of its pig-associated

446 strains. (D) Hierarchical bubble plot of the 61 pig-associated ceBGs as in panel C. The sizes of the

447 circles are proportional to the number of strains, the three levels in the plot represent (from outer to

448 inner) clusters at the levels of subspecies (HC2850), super-lineage (HC2000), and ceBG (HC900),

449 as described previously⁹. Pie charts represent the proportions of strains from different sources. The 9

450 pig-enriched ceBGs each with $>40\%$ pig strains were labelled in parts C and D.

451 **Fig. 2 | Population dynamics, ARGs, and global transmissions of ceBG1272 (*Choleraesuis*). (A) The**

452 maximum-likelihood phylogeny (left), metadata (middle), and predicted ARGs for all strains in

453 ceBG1272. The predicted lineages, clades, and clusters are labeled near the associated branches. The

454 associations between the numbers of predicted ARGs and the sampling years, source categories, and

455 countries are also visualized. (B) The associations between the numbers of predicted ARGs and the

456 sampling years in Para C lineages, and (C) the association between the number of ARGs per strain and

457 host sources. (D) Visualization of the correlations between the numbers of predicted ARGs and countries

458 in *Choleraesuis*. (E, F, and G) Bayesian inferences of the population dynamics of ceBG1272 over the past

459 ~ 2500 years. (E) Global transmission of ceBG1272. Pie charts show the proportional composition of

460 clades in each major country, and the arrows show the transmissions reconstructed based on the tree in

461 part F, with the transmission dates shown nearby. The world map was modified from the map hosted in

462 the d3.js (<https://d3js.org/>). The piecharts and arrows were color-coded by the associated clades.

463 Inset: the Simpson diversity of clades in each geographic region in the world. (F) The maximum clade-

464 credibility (MCC) tree of ceBG1272 by BEAST2. The branches were color-coded by the most probable

465 ancestral geographic origins (as in the Key). Piecharts of all possible geographic origins were shown over

466 certain nodes where the most probable origins had $<90\%$ posterior supports. The dates of origin for some

467 branches were shown together with the 95% confidence intervals in brackets. (G) The fluctuation of

468 effective population sizes with time by the ‘skygrowth’ package in R. Arrows points to the time of three

469 major developments in the modern pig industry.

470 **Fig. 3 | Host transfers for the pig-enriched ceBGs. (A) Curves show the dynamic changes of the**

471 proportional host sources with time for each ceBG. The ancestral host associations were predicted by

472 TreeTime. The predicted median effective population sizes were also shown as black curves for
473 ceBG1272 (*Choleraesuis*) and ceBG3 (*Derby*). The period for host transfers into pigs (red) or population
474 expansions (yellow) is shown above each plot. Detailed prediction of population dynamics for all nine
475 ceBGs can also be found in Extended Data Fig. 5. (B) Proportional source of host transfers summarized
476 for all nine ceBGs in the past 50 years. Detailed host transfer data for each ceBG can be found in
477 Extended Data Fig. 6. (C) Proportional source of host transfers in the past 50 years summarized for eight
478 pig-containing ceBGs that have 5-35% pig strains, including ceBGs of 5, 8, 22, 125, 276, 709, and 1898
479 (see Fig. 1C). (B, C) The arrows show the direction of transfers and are color-coded by average
480 frequencies. The most contributing sources (B: pigs, and C: human) are highlighted with a '*'. (D)
481 Median numbers of disrupted CDSs (coding sequences) per genome with 95% confidence intervals in all
482 pig-enriched and pig-containing ceBGs.

483 **Fig. 4 | Association between the transmission of the pig-enriched ceBGs and the global trade of pig-**
484 **related products.** (A, B) Visualization of the international trade of all pork-related products (top) and the
485 transmissions of pig-enriched ceBGs (bottom). The pie charts show the relative proportions of source
486 continents for the products or pathogens to the target continents. The world map was modified from the
487 map hosted in the d3.js (<https://d3js.org/>). (C) UMAP plot of Pearson's correlations among the trade and
488 the transmission of pig-enriched salmonellae. Each colored dot in the plot shows an animal-related
489 product as in the Harvard database and the grey dots are other, non-animal products. The triangle shows
490 inter-continental transmission data summarized from all pig-enriched salmonellae. The insert highlights
491 the dashed box in the plot, with arrows specifying the correlation coefficient (R) between the
492 transmissions of pathogens and the trade of pig-related products. (D-G) Linear regressions of different
493 categories of pig-related products (X-axis) and the inter-continental transmissions of pig-enriched ceBGs
494 (Y-axis). The correlation coefficient values for the linear regressions are also shown.

495 **Fig. 5 | The influences of modern agriculture on population dynamics of *Salmonella enterica***
496 **serovars.** This image provides a visual summary of the paper. Agricultural production has become
497 increasingly modernized over the past half-century. On the one hand, the pattern of large-scale intensive
498 pig farming has led to the emergence and population expansion of pig-enriched *Salmonella*; on the other
499 hand, globalized trade exchanges concerning pigs have similarly increased the probability of global
500 transmission of pig-enriched *Salmonella enterica* serovars. In addition, with the use of antibiotics in the
501 process, more and more pig-enriched *Salmonella* has obtained new antibiotic resistance genes, including
502 many of the previously reported human-specific antibiotic resistance genes. The impact of the
503 development model of modern agriculture on pig-enriched *Salmonella* is comprehensive and far-reaching.

505 **References**

- 506 1. López-Gálvez, F., Gómez, P. A., Artés, F., Artés-Hernández, F. & Aguayo, E. Interactions between
507 Microbial Food Safety and Environmental Sustainability in the Fresh Produce Supply Chain. *Foods*
508 **10**, 1655 (2021).
- 509 2. Stanaway, J. D. *et al.* The global burden of typhoid and paratyphoid fevers: a systematic analysis for
510 the Global Burden of Disease Study 2017. *Lancet Infect Dis* **19**, 369–381 (2019).
- 511 3. Bonardi, S. *Salmonella* in the pork production chain and its impact on human health in the European
512 Union. *Epidemiol. Infect.* **145**, 1513–1526 (2017).
- 513 4. Jamal, S. M. & Belsham, G. J. Foot-and-mouth disease: past, present, and future. *Vet Res* **44**, 116
514 (2013).
- 515 5. Wu, X., Fan, X., Xu, T. & Li, J. Emergency preparedness and response to African swine fever in the
516 People’s Republic of China: -EN- -FR- Préparation et réponse à la crise de peste porcine africaine en
517 République populaire de Chine -ES- Preparación para emergencias y respuesta a la peste porcina
518 africana en la República Popular de China. *Rev. Sci. Tech. OIE* **39**, 591–598 (2020).
- 519 6. Woods, A. Rethinking the History of Modern Agriculture: British Pig Production, c.1910-65. *20*
520 *Century Br Hist.* **23**, 165–191 (2012).
- 521 7. Bosse, M. *et al.* Genomic analysis reveals selection for Asian genes in European pigs following
522 human-mediated introgression. *Nat Commun* **5**, 4392 (2014).
- 523 8. Koopman, R. B., Laney, K. & Giamalva, J. Industry and Trade Summary. Publication ITS-011.
524 Washington, DC: U.S. International Trade Commission (2014).
- 525 9. Achtman, M., Zhou, Z., Charlesworth, J. & Baxter, L. EnteroBase: hierarchical clustering of 100
526 000s of bacterial genomes into species/subspecies and populations. *Phil. Trans. R. Soc. B* **377**,
527 20210240 (2022).
- 528 10. Gal-Mor, O. Persistent Infection and Long-Term Carriage of Typhoidal and Nontyphoidal
529 *Salmonellae*. *Clin Microbiol Rev* **32**, e00088-18 (2018).
- 530 11. Zhou, Z. *et al.* Pan-genome Analysis of Ancient and Modern *Salmonella enterica* Demonstrates
531 Genomic Stability of the Invasive Para C Lineage for Millennia. *Curr Biol* **28**, 2420-2428.e10 (2018).
- 532 12. Zhou, Z. *et al.* The EnteroBase user’s guide, with case studies on *Salmonella* transmissions, *Yersinia*
533 *pestis* phylogeny, and *Escherichia* core genomic diversity. *Genome Res.* **30**, 138–152 (2020).
- 534 13. Wang, R. *et al.* The global distribution and spread of the mobilized colistin resistance gene *mcr-1*.
535 *Nat Commun* **9**, 1179 (2018).
- 536 14. Shambaugh, G. E. History of Sulfonamides. *Arch Otolaryngol Head Neck Surg.* **83**, 1–2 (1966).
- 537 15. Chase-Dunn, C., Kawano, Y. & Brewer, B. D. Trade Globalization since 1795: Waves of Integration
538 in the World-System. *Am. Sociol. Rev.* **65**, 77 (2000).

- 539 16. Chiu, C.-H., Su, L.-H. & Chu, C. *Salmonella enterica* Serotype Choleraesuis: Epidemiology,
540 Pathogenesis, Clinical Disease, and Treatment. *Clin Microbiol Rev* **17**, 311–322 (2004).
- 541 17. Massei, G. *et al.* Wild boar populations up, numbers of hunters down? A review of trends and
542 implications for Europe: wild boar and hunter trends in Europe. *Pest. Manag. Sci.* **71**, 492–500
543 (2015).
- 544 18. McInnes, L., Healy, J. & Melville, J. UMAP: Uniform Manifold Approximation and Projection for
545 Dimension Reduction. Preprint at <http://arxiv.org/abs/1802.03426> (2020).
- 546 19. Dame-Korevaar, A., Boumans, I. J. M. M., Antonis, A. F. G., Van Klink, E. & De Olde, E. M.
547 Microbial health hazards of recycling food waste as animal feed. *Future Foods* **4**, 100062 (2021).
- 548 20. Aparicio, G., González-Esteban, Á. L., Pinilla, V. & Serrano, R. The World Periphery in Global
549 Agricultural and Food Trade, 1900–2000. *Agricultural Development in the World Periphery* 63–88
550 (2018).
- 551 21. Gale, F., Marti, D. & Hu, D. China’s Volatile Pork Industry. *Economic research service report*,
552 *United States Department of Agriculture*, pp. 1-27(2012).
- 553 22. Simon, S. Real People, Real Dogs, and Pigs for the Ancestors: The Moral Universe of
554 “Domestication” in Indigenous Taiwan: Real People, Real Dogs, and Pigs for the Ancestors. *Am*
555 *Anthropol.* **117**, 693–709 (2015).
- 556 23. Luhmann, N., Holley, G. & Achtman, M. BlastFrost: fast querying of 100,000s of bacterial genomes
557 in Bifrost graphs. *Genome Biol* **22**, 30 (2021).
- 558 24. Chiu, C.-H. *et al.* The Emergence in Taiwan of Fluoroquinolone Resistance in *Salmonella enterica*
559 Serotype Choleraesuis. *N Engl J Med* **346**, 413–419 (2002).
- 560 25. Bawn, M. *et al.* Evolution of *Salmonella enterica* serotype Typhimurium driven by anthropogenic
561 selection and niche adaptation. *PLoS Genet* **16**, e1008850 (2020).
- 562 26. Key, F. M. *et al.* Emergence of human-adapted *Salmonella enterica* is linked to the Neolithization
563 process. *Nat Ecol Evol* **4**, 324–333 (2020).
- 564 27. Sévellec, Y. *et al.* Polyphyletic Nature of *Salmonella enterica* Serotype Derby and Lineage-Specific
565 Host-Association Revealed by Genome-Wide Analysis. *Front. Microbiol.* **9**, 891 (2018).
- 566 28. Comas, I. *et al.* Out-of-Africa migration and Neolithic coexpansion of *Mycobacterium tuberculosis*
567 with modern humans. *Nat Genet* **45**, 1176–1182 (2013).
- 568 29. Roasto, M. *et al.* *Salmonella enterica* prevalence, serotype diversity, antimicrobial resistance and
569 control in the European pork production chain. *Trends Food Sci Technol* **131**, 210–219 (2023).
- 570 30. Dawoud, T. M., Shi, Z., Kwon, Y. M. & Ricke, S. C. Overview of Salmonellosis and Food-borne
571 *Salmonella*. *Producing Safe Eggs* 113–138 (2017).
- 572 31. Werber, D. *et al.* International outbreak of *Salmonella* Oranienburg due to German chocolate. *BMC*
573 *Infect Dis* **5**, 7 (2005).
- 574 32. Sokurenko, E. V., Gomulkiewicz, R. & Dykhuizen, D. E. Source–sink dynamics of virulence
575 evolution. *Nat Rev Microbiol* **4**, 548–555 (2006).

- 576 33. Li, S., He, Y., Mann, D. A. & Deng, X. Global spread of *Salmonella* Enteritidis via centralized
577 sourcing and international trade of poultry breeding stocks. *Nat Commun* **12**, 5109 (2021).
- 578 34. Foreyt, W. J. *Trichinosis: Reston, Va., U.S. Geological Survey Circular 1388, 60 p., 2 Appendixes.*
579 (2013).
- 580 35. Leekitcharoenphon, P. *et al.* Cross-Border Transmission of *Salmonella* Choleraesuis var. Kunzendorf
581 in European Pigs and Wild Boar: Infection, Genetics, and Evolution. *Front. Microbiol.* **10**, 179
582 (2019).
- 583 36. Achtman, M. *et al.* Genomic diversity of *Salmonella enterica* -The UoWUCC 10K genomes project.
584 *Wellcome Open Res* **5**, 223 (2021).
- 585 37. Key, F. M. *et al.* Emergence of human-adapted *Salmonella enterica* is linked to the Neolithization
586 process. *Nat Ecol Evol* **4**, 324–333 (2020).
- 587 38. Bankevich, A. *et al.* SPAdes: A New Genome Assembly Algorithm and Its Applications to Single-
588 Cell Sequencing. *J Comput Biol* **19**, 455–477 (2012).
- 589 39. Seemann, T. Prokka: rapid prokaryotic genome annotation. *Bioinformatics* **30**, 2068–2069 (2014).
- 590 40. Cantalapiedra, C. P., Hernández-Plaza, A., Letunic, I., Bork, P. & Huerta-Cepas, J. eggNOG-mapper
591 v2: Functional Annotation, Orthology Assignments, and Domain Prediction at the Metagenomic
592 Scale. *Mol Biol Evol* **38**, 5825–5829 (2021).
- 593 41. Bortolaia, V. *et al.* ResFinder 4.0 for predictions of phenotypes from genotypes. *J Antimicrob*
594 *Chemother* **75**, 3491–3500 (2020).
- 595 42. Zhou, Z., Charlesworth, J. & Achtman, M. Accurate reconstruction of bacterial pan- and core
596 genomes with PEPPAN. *Genome Res.* **30**, 1667–1679 (2020).
- 597 43. Nguyen, L.-T., Schmidt, H. A., Von Haeseler, A. & Minh, B. Q. IQ-TREE: A Fast and Effective
598 Stochastic Algorithm for Estimating Maximum-Likelihood Phylogenies. *Mol Biol Evol* **32**, 268–274
599 (2015).
- 600 44. Didelot, X., Croucher, N. J., Bentley, S. D., Harris, S. R. & Wilson, D. J. Bayesian inference of
601 ancestral dates on bacterial phylogenetic trees. *Nucleic Acids Res.* **46**, e134–e134 (2018).
- 602 45. Rambaut, A., Lam, T. T., Max Carvalho, L. & Pybus, O. G. Exploring the temporal structure of
603 heterochronous sequences using TempEst (formerly Path-O-Gen). *Virus Evol* **2**, vew007 (2016).
- 604 46. Letunic, I. & Bork, P. Interactive Tree Of Life (iTOL) v4: recent updates and new developments.
605 *Nucleic Acids Res.* **47**, W256–W259 (2019).
- 606 47. Bouckaert, R. *et al.* BEAST 2: A Software Platform for Bayesian Evolutionary Analysis. *PLoS*
607 *Comput Biol* **10**, e1003537 (2014).
- 608 48. Sagulenko, P., Puller, V. & Neher, R. A. TreeTime: Maximum-likelihood phylodynamic analysis.
609 *Virus Evol* **4**, (2018).
- 610 49. Becht, E. Dimensionality reduction for visualizing single-cell data using UMAP. *Nat Biotechnol* **37**,
611 38–44 (2019).

612

613

614

615 **Extended Data Figure 1. Circular presentation of the maximum-likelihood phylogeny in Figure 1A.**

616 Outer rings: The clade, source, and geographic origin of each strain. Colored arcs underneath the tree
617 show the cluster assignments as in the Key.

618 **Extended Data Figure 2. Evaluation of the presence of temporal signal in *S. enterica* serovar**

619 **Choleraesuis.** The analysis was performed on 587 genomes. (A) Linear regression between root-to-tip
620 distances of strains and the sampling years with a coefficient of determination (R^2) of 0.67. (B)
621 Substantially lower R^2 values were obtained for ten date-randomisation datasets. (C) The average (dots)
622 and standard deviation (error bars) of the substitution rates for actual data (black) and ten date-
623 randomisation datasets (red), estimated by BactDating.

624 **Extended Data Figure 3. Assessing the existence of temporal signal randomization test in pig-**

625 **enriched ceBGs.** (A) Coefficients of determination (R^2) for the ten date-randomisation tests were
626 obtained by linear regression between root-to-tip distances of strains and the sampling years in pig-
627 enriched ceBGs. (B) The average (dots) and standard deviations (error bars) of the substitution rates for
628 actual data (black) and ten date-randomisation datasets (red) by BactDating. Pig-enriched ceBGs
629 including ceBG3 (n=3136), ceBG10 (n=622), ceBG17 (n=155), ceBG35 (n=516), ceBG37 (n=1012),
630 ceBG40 (n=176), ceBG459 (n=1441), ceBG621 (n=787), ceBG1272 (n=586). The ancient sample was
631 not included in ceBG1272 in both (A) and (B).

632 **Extended Data Figure 4. The geographic states of the ancestral nodes in the Choleraesuis**

633 **population after downsamplings.** (A) Downsampling tests of up to ten strains per country/region. (B)
634 Downsampling tests of up to five strains per country/region. Both: the geographic states were predicted
635 using TreeTime. Each test was run in 100 parallels. The pie charts illustrate the proportions of the best-
636 supported geographic states in the 100 parallels for the corresponding ancestral nodes.

637 **Extended Data Figure 5. Reconstructed ancestral host associations for all nodes in nine pig-**

638 **enriched ceBGs.** The corresponding ceBGs for each panel are: (A) ceBG3 (Derby), (B) ceBG1272
639 (Choleraesuis), (C) ceBG17 (Chailey), (D) ceBG35 (Worthington), (E) ceBG37 (London), (F) ceBG40
640 (Cerro), (G) ceBG459 (Johannesburg), (H) ceBG621 (Ohio), (I) ceBG10 (Adelaide). The mean values of
641 effective population sizes with time were also shown for (A) and (B), with 95% confidence intervals in
642 grey shapes. The orange and grey boxes show the periods of population expansion (A, B) or the periods
643 of host transfers into pigs (C-I).

644 **Extended Data Figure 6. The host transmission frequency of nine pig-enriched ceBGs.** The

645 corresponding ceBGs for each panel are: (A) ceBG10 (Adelaide), (B) ceBG1272 (Choleraesuis), (C)

646 ceBG17 (Chailey), (D) ceBG3 (Derby), (E) ceBG35 (Worthington), (F) ceBG37 (London), (G) ceBG 40
647 (Cerro), (H) ceBG 459 (Johannesburg), (I) ceBG 621 (Ohio). Different arrows represent the direction of
648 host transmission, with darker colors indicating higher transfer frequency. “*” marks the most
649 contributing host sources for the transmissions.

650 **Extended Data Figure 7. A 5 X 5 table showing the summarised international transmission events**
651 **of all nine pig-enriched ceBGs in *Salmonella* in the past 50 years.** The maximum-likelihood phylogeny
652 was reconstructed based on SNPs in the core genome of each ceBG and the date of origin was estimated
653 using BactDating. TreeTime was applied to reconstruct the country sources for all nodes in the tree. A
654 transmission was recorded when the ancestral node and descending node of a branch were different. All
655 transmissions were then summarized and grouped based on their associated continents.

656 **Extended Data Figure 8. Pearson’s correlations analysis of sub-classification for pig-related**
657 **products.** The Sub classifications involved include (A) Pork offal, frozen (021011); (B) Pork, frozen
658 (020649); (C) Pork, frozen cut (020329); (D) Pork, preserved (020322); (E) Pork offal, fresh (020630);
659 (F) Pig fat (020910); (G) Pork, fresh cut (020912); (H) Pork, fresh (020319); (I) Pig carcasses
660 (020310); (J) Pig, live breeding (010391); (K) Pig, live, less 50kg (010392); (L) Pig, live, over 50kg
661 (020311). The codes in parentheses represent the Harmonized System Codes of the products. Analyzing
662 the correlation between the intercontinental dissemination of each pig-related commodity and the
663 intercontinental transmission of pig-enriched ceBGs. R: Pearson’s correlation coefficient.

664

665 **Supplementary Information and Additional Supplementary Files**

666

667 **Supplementary Table S1. Pig-enriched HC5s that were isolated from multiple countries.**

668 The item in the table including the HC5 cluster from Enterobase, corresponded with pig-enriched ceBGs,
669 continent, transnational, and host sources information.

670

671 **Supplementary Table S2. Simpson's diversity of clades at the national level.**

672 When calculating the Simpson’s diversity of clades, only countries with more than 10 strains
673 were selected.

674

675 **Supplementary Table S3. Distribution of the colistin-resistant genes in serovars *Choleraesuis*.**

676 Information on colistin-resistant genes extracted from the statistical information on the number of ARGs
677 of strains of serovar *Choleraesuis* is summarised in this table. The collection years, host sources, and
678 geographic information for strains with colistin resistance are labeled in the table.

679

680 **Supplementary Table S4. The frequencies of transmissions in each pair of regions across all**
681 **100 random downsamplings.**

682 The table on the left shows the results of 5 samples drawn from each region, while the table on
683 the right shows the results of 10 samples drawn from each region. The transmission frequency
684 corresponds to the total number of transmission events that occur in 100 repeats.

685

686 **Additional Supplementary Files Table 1 Metadata of eight pig-enriched ceBGs except 1272**
687 **(Choleraesuis).**

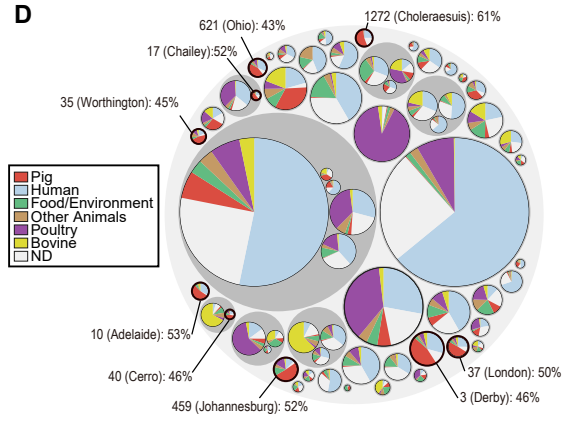
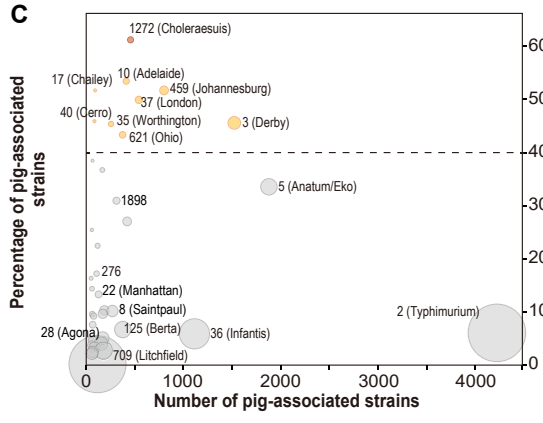
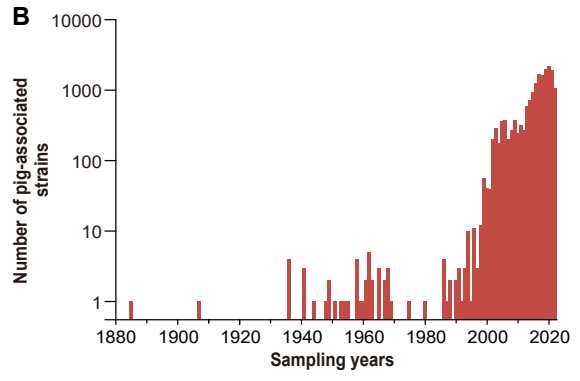
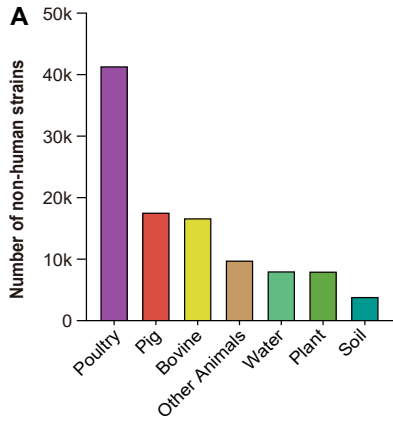
688 The metadata included eight pig-enriched ceBGs (which had $\geq 40\%$ of the strains from pigs) except
689 ceBG1272 (Choleraesuis), including ceBG3 (Derby), ceBG10 (Adelaide), ceBG459 (Johannesburg),
690 ceBG37 (London), ceBG621 (Ohio), ceBG40 (Cerro), ceBG35 (Worthington), and ceBG17 (Chailey).

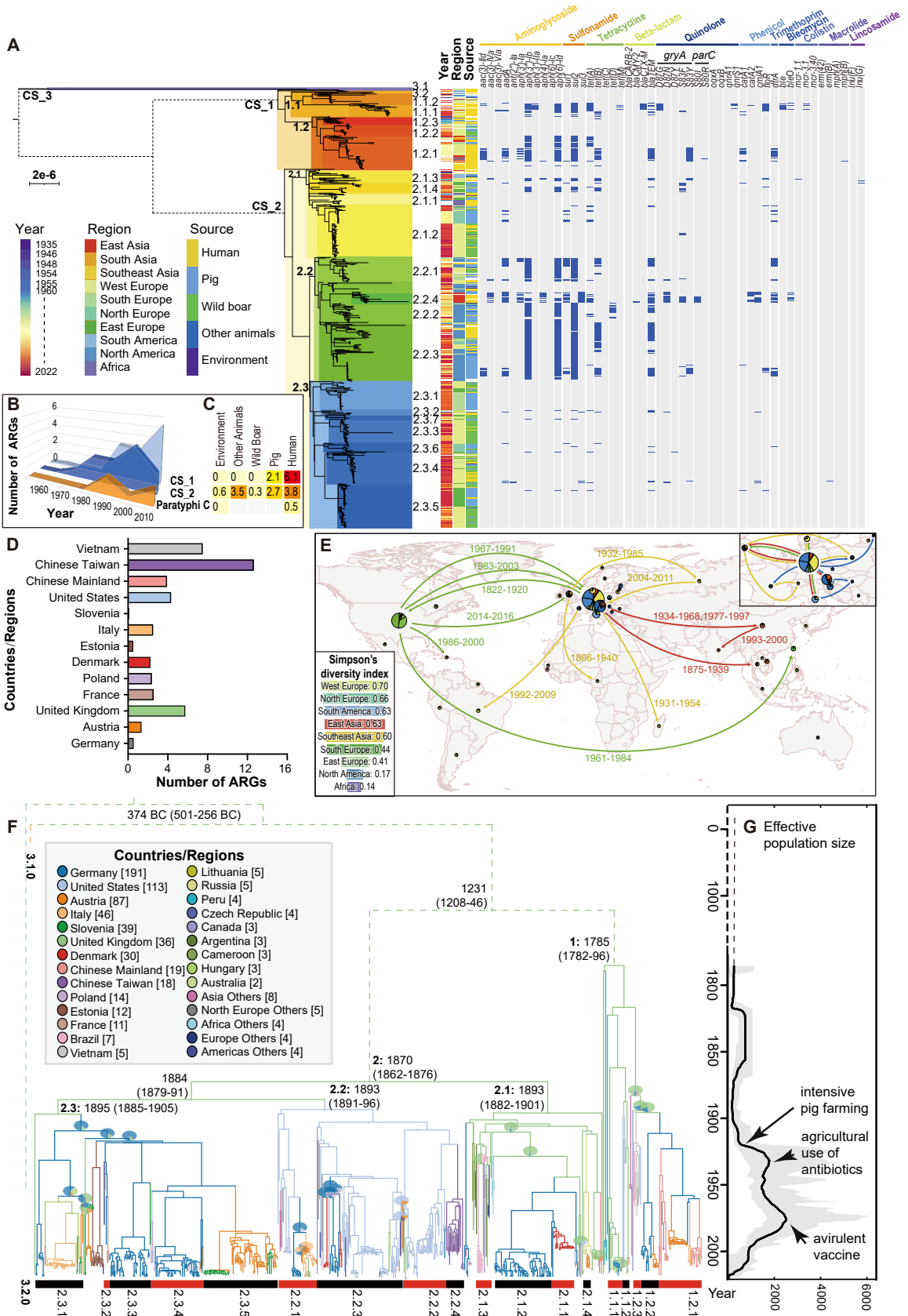
691 The table provides information about the ceBG names, geographic information, collection year, source
692 details, and the number of ARGs per strain of these pig-enriched ceBGs.

693

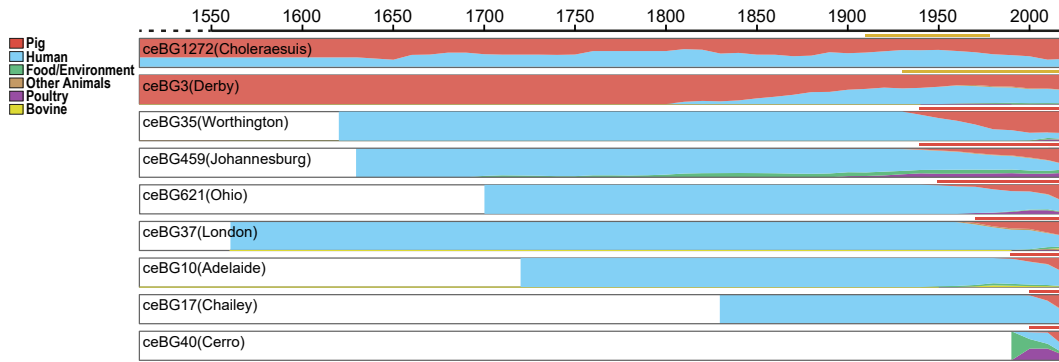
694 **Additional Supplementary Files Table 2 Metadata of *Salmonella* strains in the serovars**

695 **Choleraesuis and Paratyphi C.** There is a total of 911 *Salmonella* strains from the Para C lineage,
696 including 757 *S. Choleraesuis* serovars and 154 Paratyphi C serovars. The specific serotyping, geographic
697 information, collection year, and host source details of these strains are listed in this table, as well as the
698 statistical information about the number of ARGs per strain.

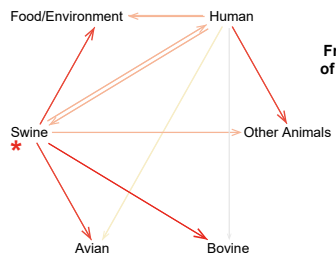




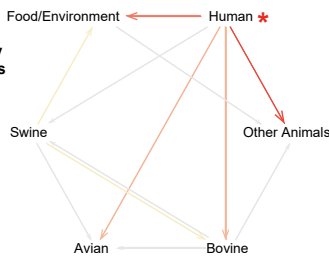
A Predicted host association with time



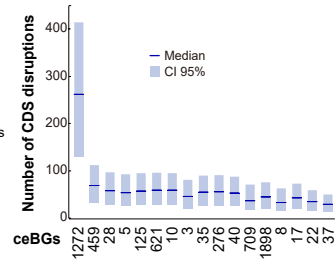
B Pig-enriched ceBGs



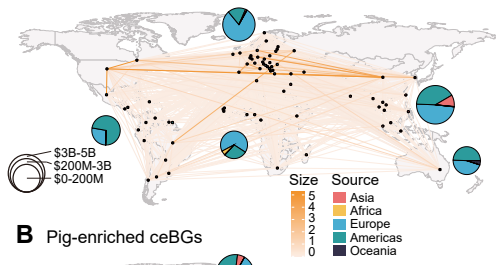
C Pig-containing ceBGs



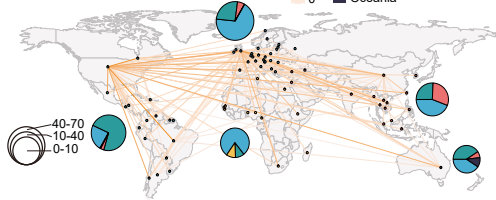
D



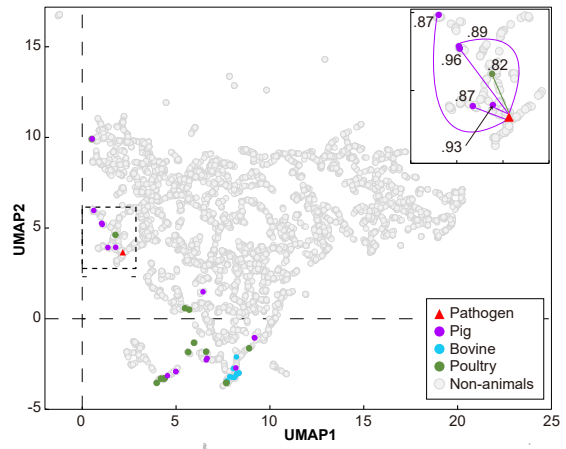
A Pork-related products



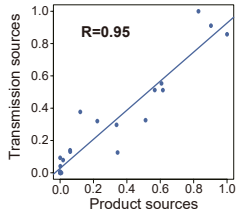
B Pig-enriched ceBGs



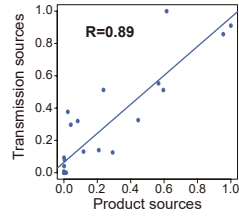
C



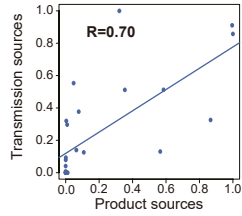
D Pork frozen



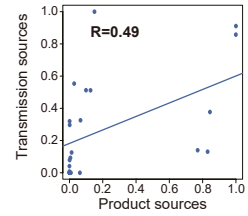
E Pork processed



F Pork fresh



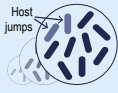
G Pig live






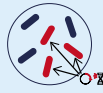
Modern Agriculture


Intensive
Pig Farming



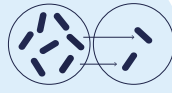
Establishment and expansion
of pig-enriched *Salmonella*


Antimicrobial
Overuse

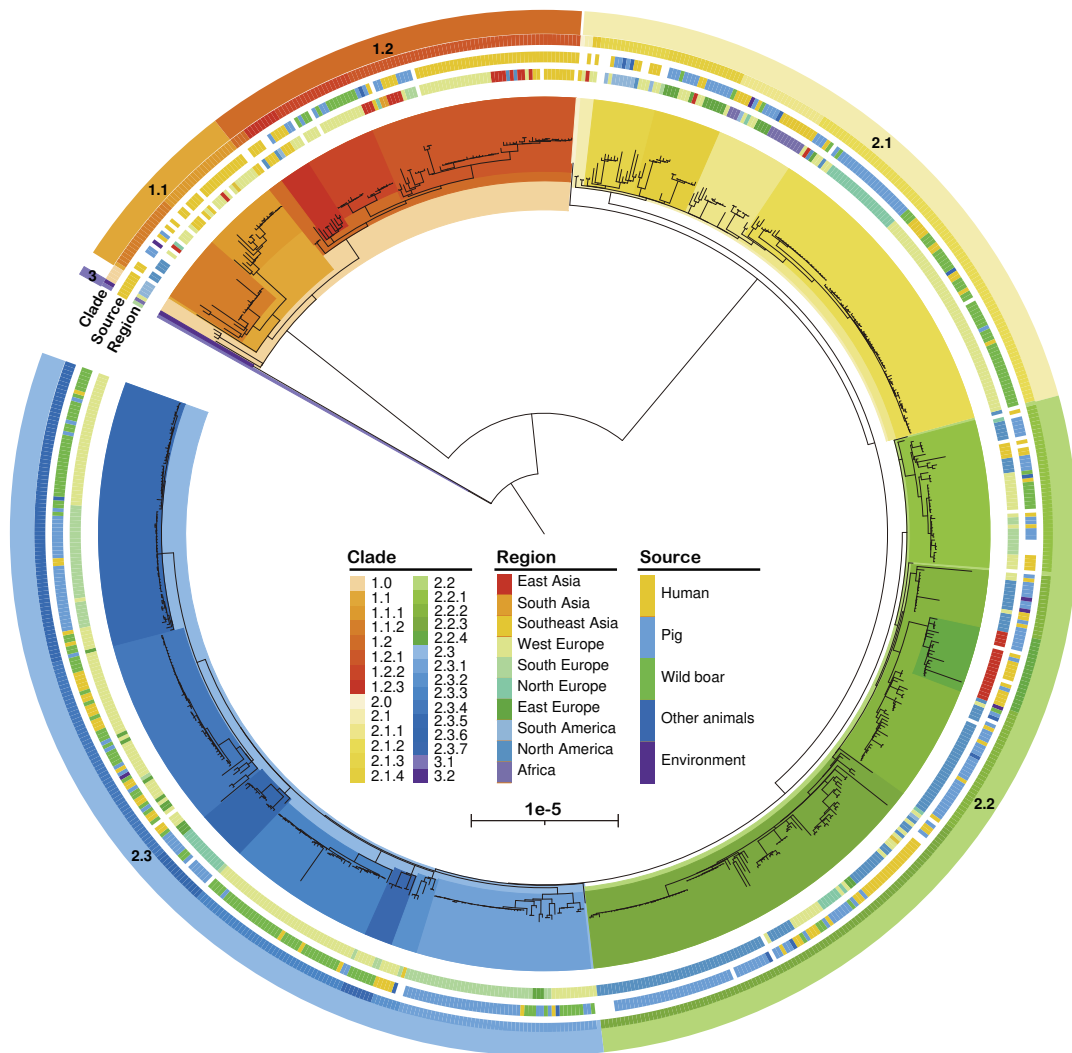


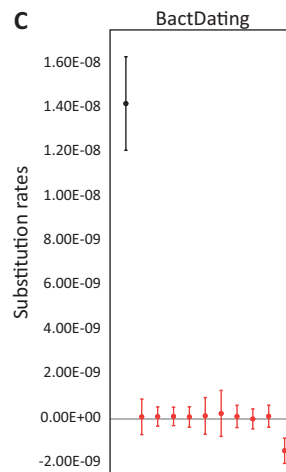
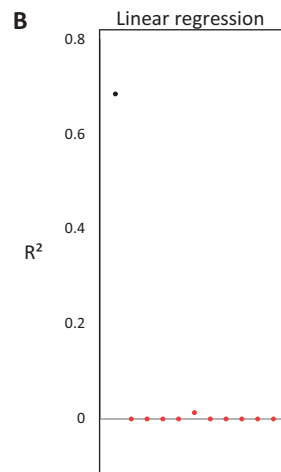
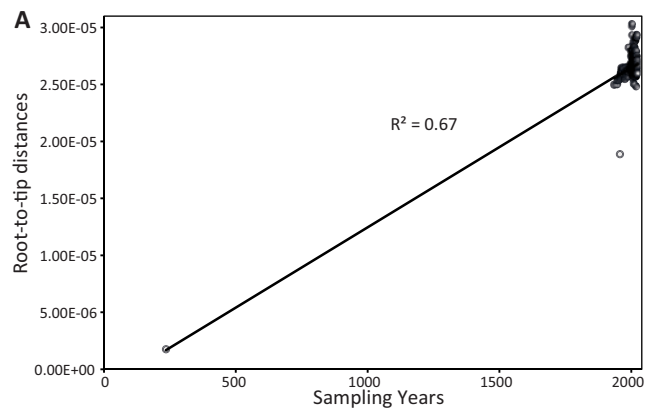
Increase of
AMR level

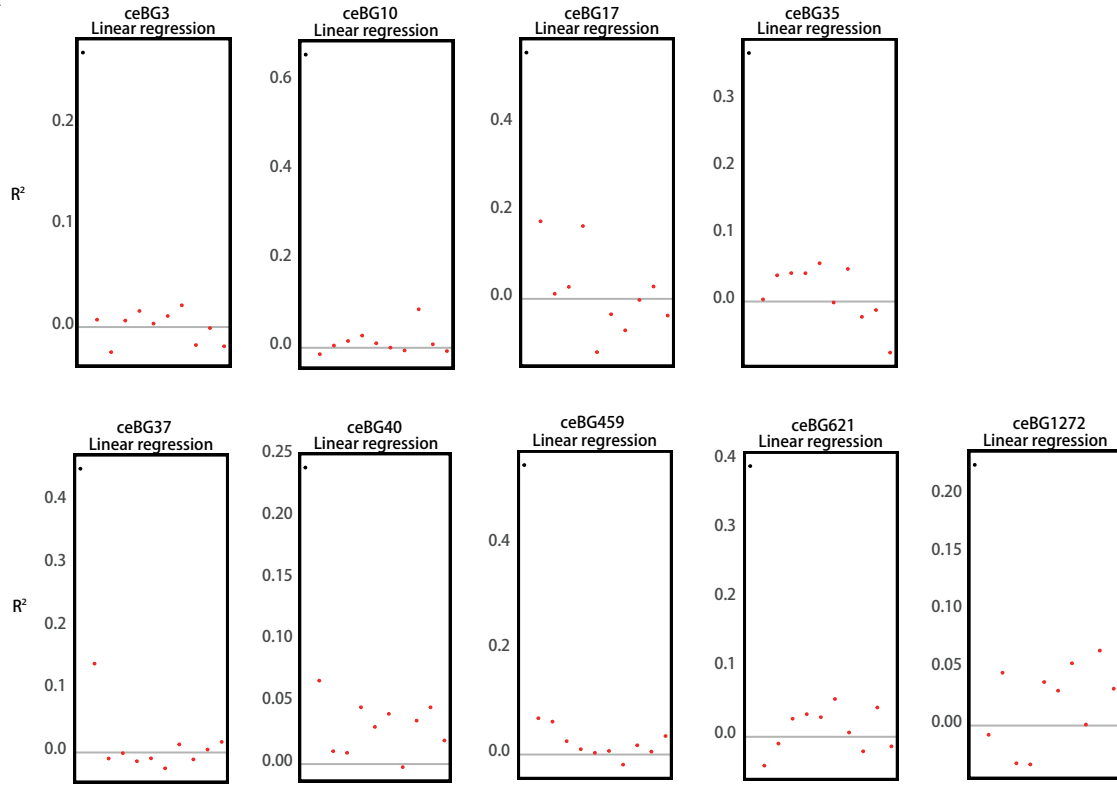
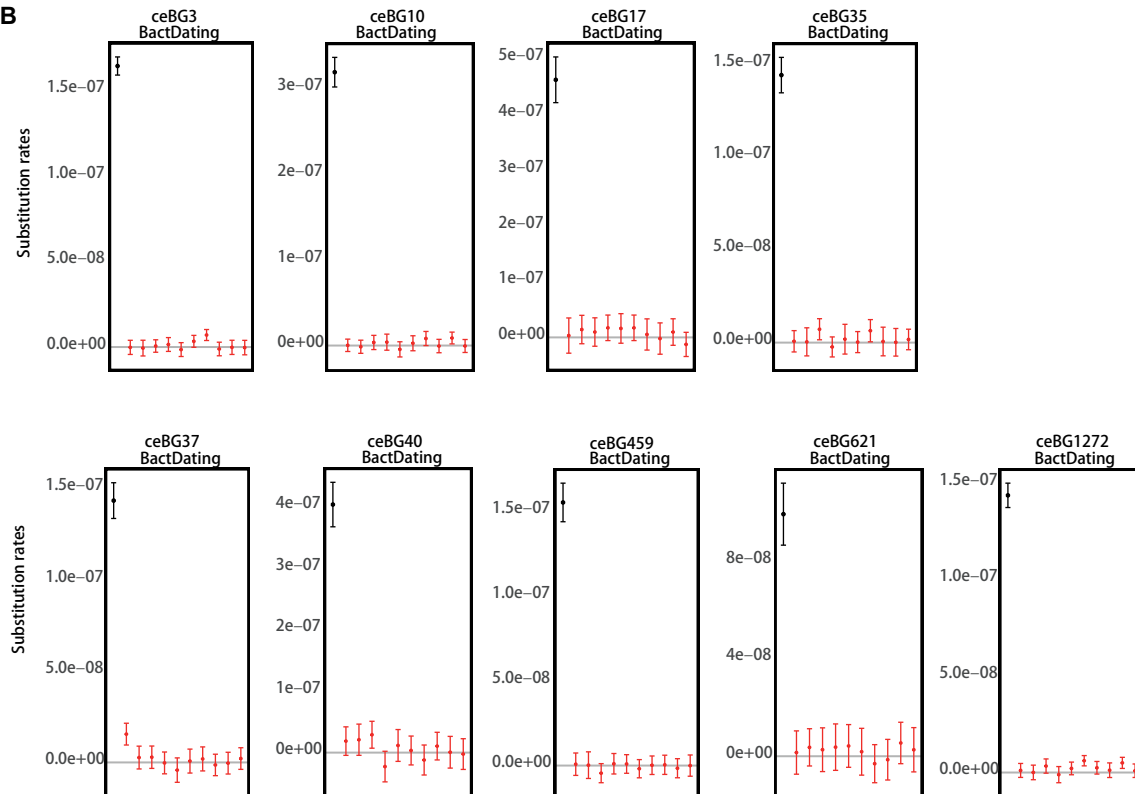

Global
Transportation



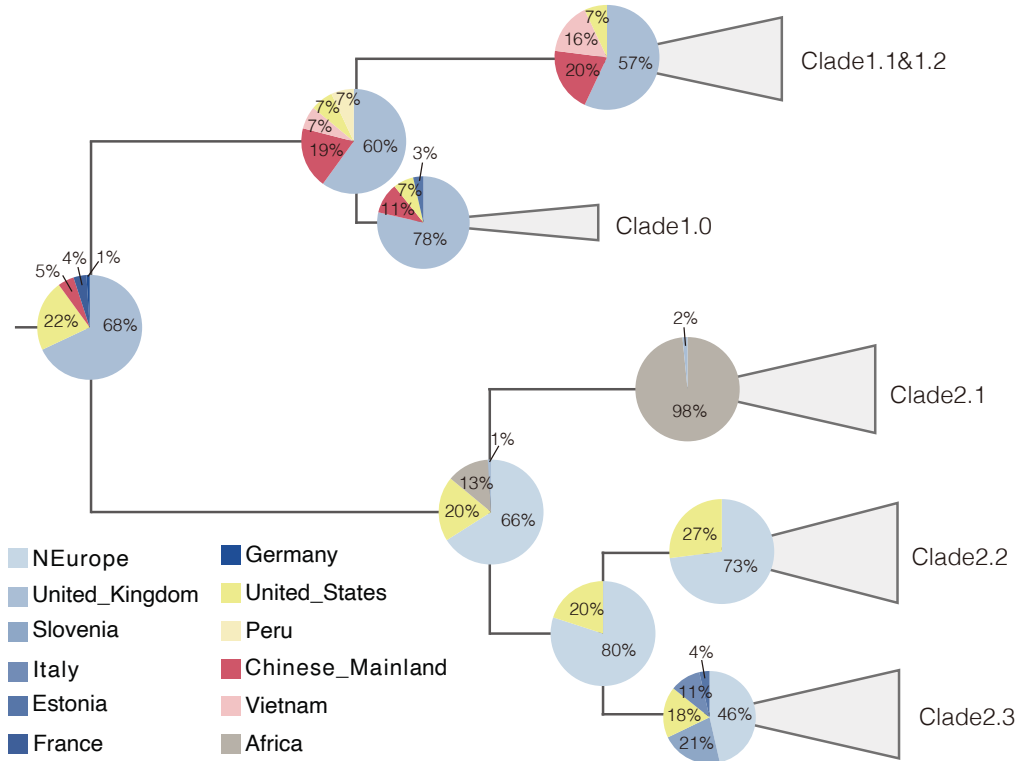
Increase of
international transmissions



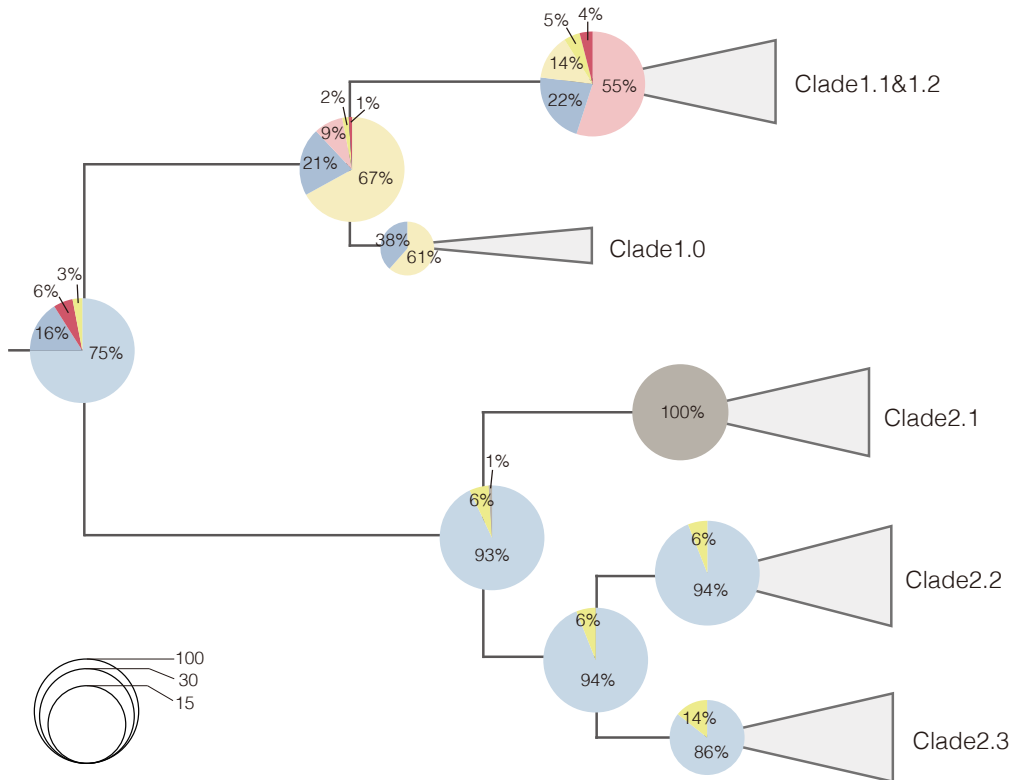


A**B**

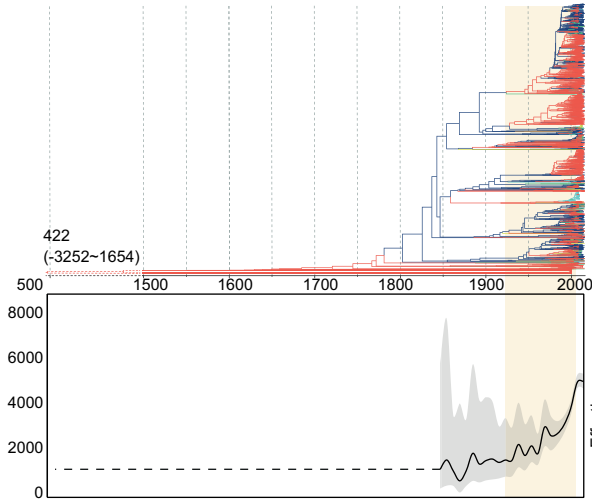
A Random sampling of 10 isolates from each country /region



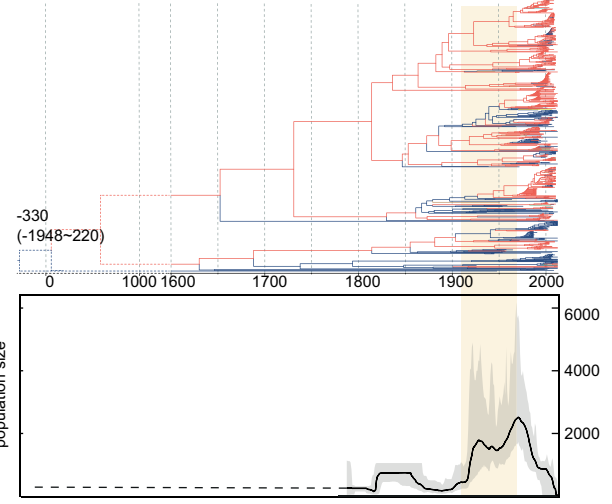
B Random sampling of 5 isolates from each country /region



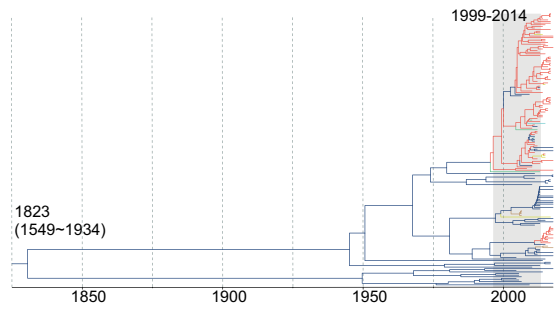
A ceBG3(Derby)



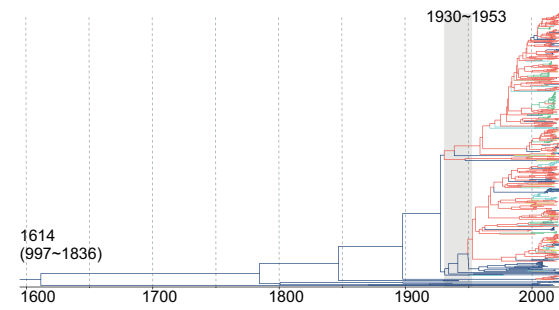
B ceBG1272(Choleraesuis)



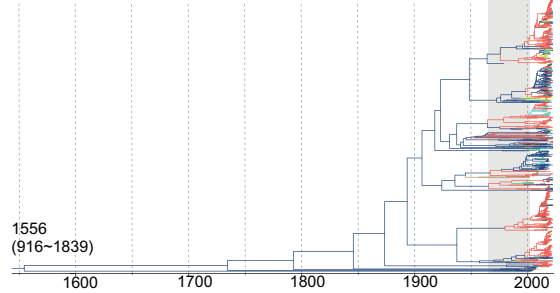
C ceBG17(Chailey)



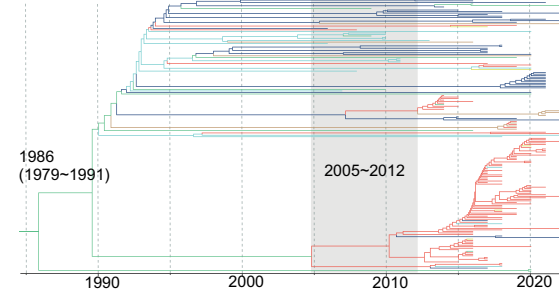
D ceBG35(Worthington)



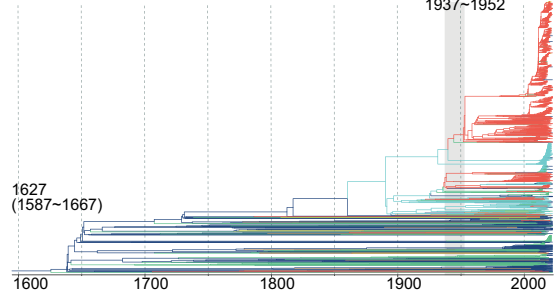
E ceBG37(London)



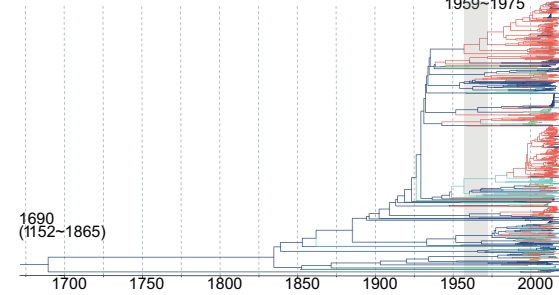
F ceBG40(Cerro)



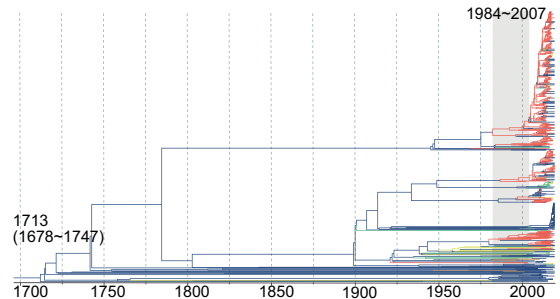
G ceBG459(Johannesburg)

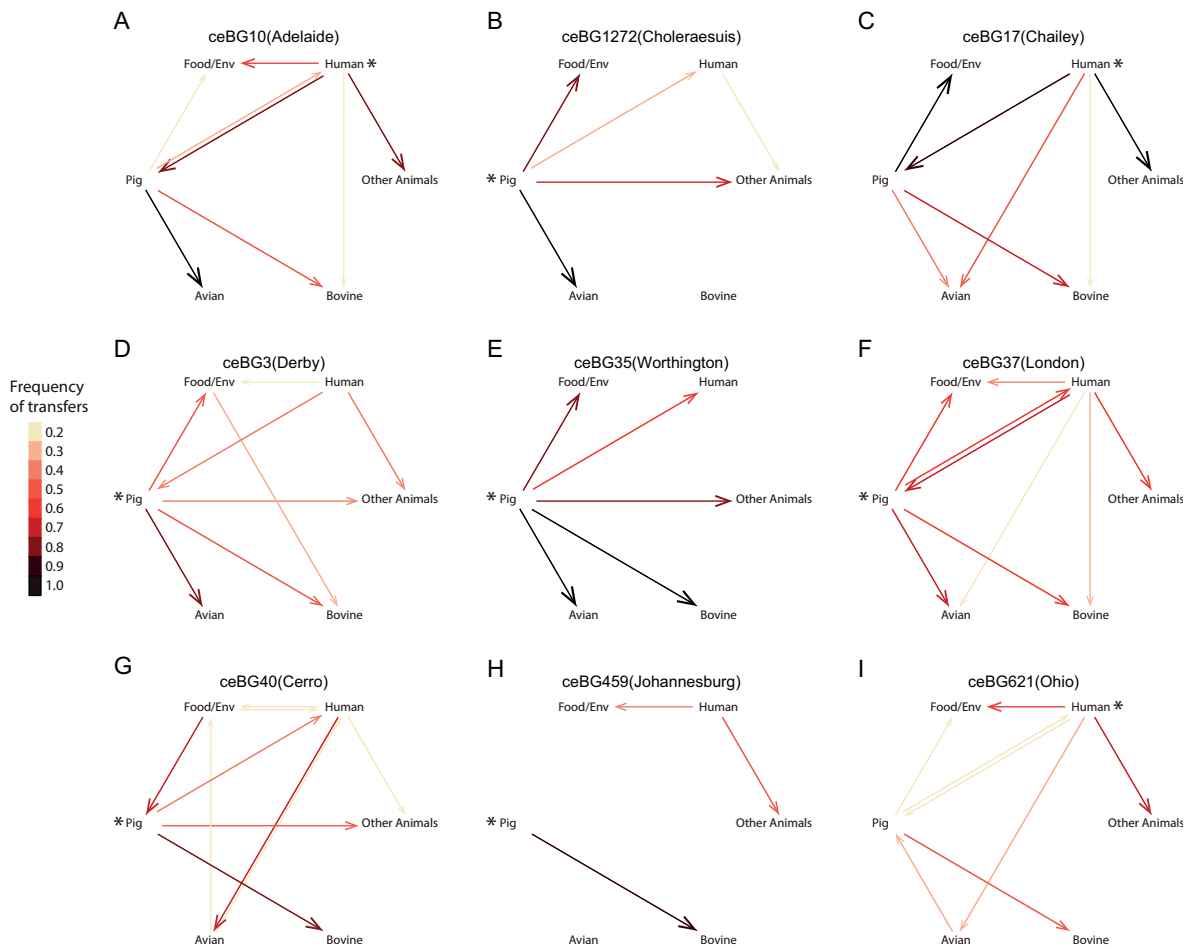


H ceBG621(Ohio)



I ceBG10(Adelaide)





		Source				
		Africa	Asia	Europe	Americas	Oceania
Target	Africa	2.077	0.000	15.922	2.000	0.000
	Asia	0.000	12.301	18.062	10.634	0.000
	Europe	0.006	4.643	50.505	18.841	0.000
	Americas	0.325	1.825	13.220	40.602	0.025
	Oceania	0.000	0.663	3.672	3.665	1.000

